# Modeling and Control of a Hybrid Magnetic Bearing in a Ring-type Flywheel System

Chow-Shing Toh[a] and Shyh-Leh Chen[b]

[a] Department of Mechanical Engineering and Advanced Institute of Manufacturing with High-tech Innovations, National Chung Cheng University, Chiayi 621, Taiwan, dennis_tcs@hotmail.com
[b] Department of Mechanical Engineering and Advanced Institute of Manufacturing with High-tech Innovations, National Chung Cheng University, Chiayi 621, Taiwan, imeslc@ccu.edu.tw

***Abstract*—In this study, a hybrid magnetic bearing (HMB) is proposed for a ring-type flywheel system. The HMB is composed of passive and active units. The rotor weight will be fully supported by the lateral forces of the passive units. The other 4 DOFs will be levitated and controlled by the active units. We will first establish the magnetic force model of the passive and active units of the proposed HMB. With the magnetic force models in hand, a stabilizing levitation controller for the HMB is designed. Moreover, numerical simulation results verify the effectiveness of the controller.**

## I. INTRODUCTION

Magnetic bearing is an important type of noncontact bearing. It possesses the advantages of no friction, less energy loss, and environmental friendliness [1, 2]. Therefore, they can find wide applications, such as those requiring high speed. In general, there are three types of magnetic bearings: passive, active, and hybrid. Passive magnetic bearing (PMB) has the advantage of no energy consumption, but cannot be used alone for stable levitation. Stable levitation can be achieved by the active magnetic bearing (AMB) that uses the electromagnets to actively control the magnetic forces, with the disadvantage of higher cost and energy consumption. Hybrid magnetic bearing (HMB) is an integration of PMB and AMB. In other words, some degree-of-freedoms (DOF) of the rotor are levitated by PMB and the other DOFs are levitated by AMB.

The objective of this study is to propose an HMB for a ring-type flywheel system [3]. The HMB is composed of passive and active units. The rotor weight will be fully supported by the lateral forces of the passive units. The other 4 DOFs will be levitated and controlled by the active units. We will first establish the magnetic force model of the passive and active units of the proposed HMB. With the magnetic force model, we can then design a stabilizing controller for the HMB for stable levitation of a rigid rotor. For the passive unit, the magnetic force is a function of the air gap and offset between the stator and rotor Halbach arrays 4, 5]. For the active unit, the magnetic force is a function of the air gap and the coil current. With the magnetic force models in hand, a stabilizing levitation controller for the HMB will be designed. Numerical simulation will be conducted to verify the effectiveness of the controller.

## II. DESCRIPTION OF HMB

In this study, a novel type of HMB is proposed, which consists of active and passive magnetic units. For the passive unit, both the rotor and stator sides are equipped with Halbach array of permanent magnets, as shown in Fig. 1. For the active unit, the stator is composed of a permanent magnet and two electromagnets and the rotor consists of the Halbach array of permanent magnets, as shown in Fig. 2. The two electromagnets are wound together in a differential way so that the coil currents will be provided with the differential driving. As a result, the stator will work as a Halbach array, but its magnetic field can be actively controlled.

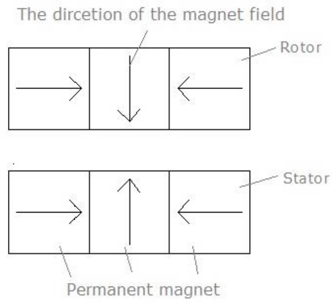


Fig. 1 The passive unit of the HMB

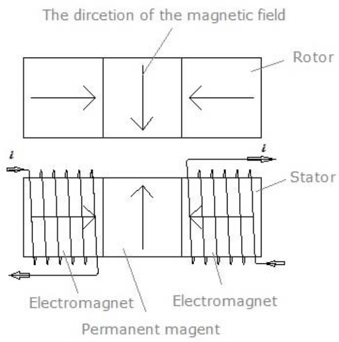


Fig. 2 The active unit of the HMB

III. MAGNETIC FORCE MODEL

The analytical magnetic force models will be obtained experimentally. For each magnetic unit, there exist normal magnetic force and lateral magnetic force. We denote them by $f_{pn}$ and $f_{pl}$, respectively, for the passive magnetic unit; and $f_{an}$ and $f_{al}$, respectively, for the active magnetic unit. For the passive magnetic unit, the magnetic forces are functions of air gap ($l$) and offset ($s$). Please refer to Fig. 3 for the definition of air gap and offset. For the active magnetic unit, the magnetic forces are functions of air gap and coil current ($i$). It is assumed that the offset in the active magnetic unit is negligible. In summary, the following four functions will be obtained experimentally

normal force of passive unit: $f_{pn}(l, s)$

lateral force of passive unit: $f_{pl}(l, s)$

normal force of active unit: $f_{an}(l, i)$

lateral force of active unit: $f_{al}(l, i)$

For each pair of air gap, offset (for passive unit only), and coil current (for active unit only), both the normal and lateral magnetic forces are measured using a load cell, as shown in Fig. 3 for the measurement of normal force and Fig. 4 for the measurement of lateral force.

Fig. 5 shows several sets of measurement data for $f_{pn}(l, s)$. With the experimental data, the least square based curve fitting method will be employed to obtain the magnetic force model $f_{pn}(l, s)$. Since the magnetic force model is a function of multiple variables, it is difficult to choose a proper candidate function for curve fitting. It is found that for each air gap, if the magnetic forces are normalized with respect to the maximum force, the magnetic forces with distinct air gaps almost coincide, as shown in Fig. 6. In other words, it is independent of air gap. This implies that the magnetic force model can be expressed as a function of separate variables. That is, it is a multiplication of two single-variable functions, the function of air gap and that of offset. In other words,

$$f_{pn}(l, s) \approx k f_{pn1}(l) f_{pn2}(s)$$

The two functions can be obtained using the technique of curve fitting separately. The polynomial functions of least degree are used for curve fitting.

Similar technique can be applied to obtain the other magnetic force models: $f_{pl}(l, s)$, $f_{an}(l, i)$, and $f_{al}(l, i)$. The details will be presented in the full-length paper.

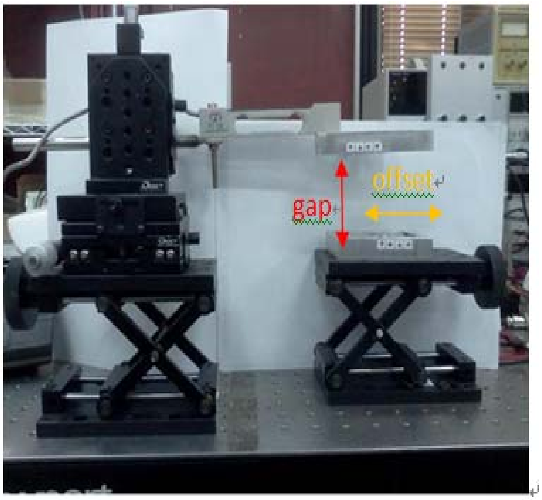


Fig. 3 Measurement set-up for normal force of the passive unit

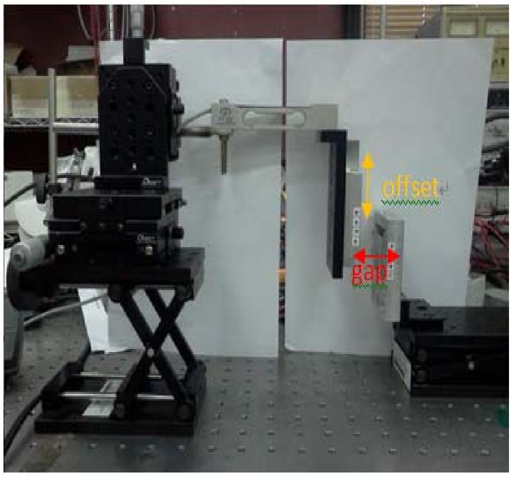


Fig. 4 Measurement set-up for lateral force of the passive unit

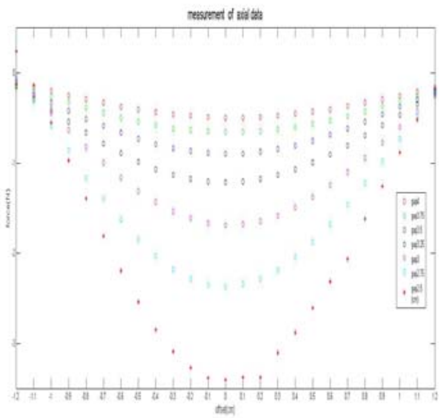

Fig. 5 Measurement of normal force for the passive unit

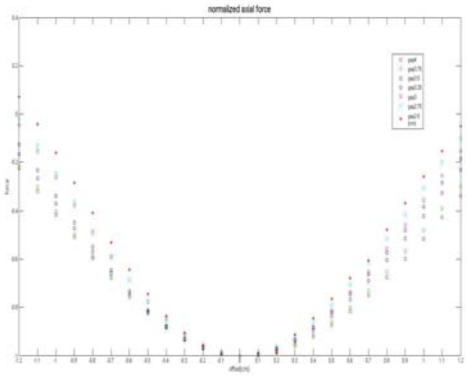

Fig. 6 Normalized normal force for the passive unit

### IV. APPLICATION TO A RING-TYPE FLYWHEEL SYSTEM

The proposed HMB is intended to be used in a ring-type flywheel system, as shown in Fig. 7. The rotor weight will be fully supported by the lateral forces of the passive units. The other 4 DOFs will be levitated and controlled by the active units. The magnetic force models established in the previous sections can be generalized to the ring-type HMB. With the magnetic force model, one can then get the dynamic model and design the stabilizing controller accordingly.

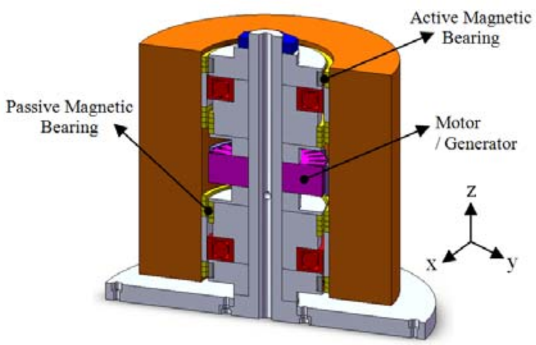


Fig. 7 The ring-type flywheel system

In the present system, an octagon structure with 8 cuboid active magnetic units is designed to form a ring-type magnetic bearing, as shown in Fig. 8. There are 8 coil sets on the stator and the opposite coil sets are wired in a differential way. As a result, there are four independent control currents in this system, and bias currents are not necessary. In other words, the magnetic force for the 4 DOFs can be approximated as

$$f_{atx} \approx k_1 i_{tx} \ , \ f_{aty} \approx k_2 i_{ty} \quad (1)$$

$$f_{abx} \approx k_3 i_{bx} \ , \ f_{aby} \approx k_4 i_{by} \quad (2)$$

where $i_{tx}$, $i_{ty}$, $i_{bx}$, $i_{by}$ are control currents and $k_1$, $k_2$, $k_3$, $k_4$ are constant. The subscript with "a" denotes AMB and subscript with "t" and "b" denotes top and bottom.

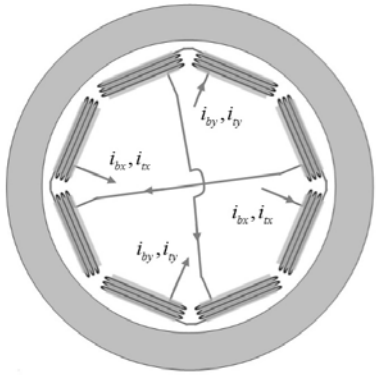


Fig. 8 An octagon structure with 8 cuboid active magnetic units

Next, the passive magnetic unit consisting of ring-type permanent magnet Halbach array is considered. Similar to the active unit, the magnetic force is formed by a deci-hexagon structure with 16 cuboid passive magnetic units, as shown in Fig. 9. When the rotor is running at the steady state, the summation force at the radial directions will be zero. The magnetic force on the passive magnetic unit can be expressed as

$$f_{pl} \approx k_{pl}(z,s) \ , \ f_{pl} \approx k_{pv}(z,s) \quad (3)$$

where $z$ is offset. Note that $k_{pl}$ and $k_{pv}$ is a parameter in terms of air gap and offset. The subscript with "p" denotes PMB and subscript with "$l$" and "$v$" denotes normal and vertical.

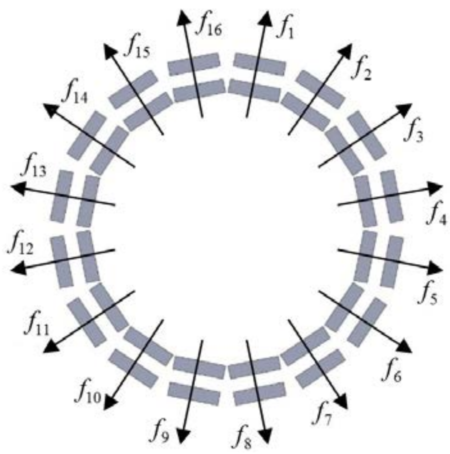


Fig. 9 A deci-hexagon structure with 16 cuboid passive magnetic units

Because the wall of ring-type magnets is quite thin and the diameters are large, the ring-type magnets are difficult to be fabricated and magnetized, so the passive unit consists of segmented arc-shaped permanent magnets.

In order to obtain the equation of motions for this flywheel battery prototype, energy method is applied here. It is assumed that the rotor displacement at $z$ -direction is small. Then, the equations of motion can be obtained and expressed as

$$\sum F_x = m\frac{l_t\ddot{x}_b + l_b\ddot{x}_t}{l_t + l_b} \quad (4)$$

$$\sum F_y = m\frac{l_t\ddot{y}_b + l_b\ddot{y}_t}{l_t + l_b} \quad (5)$$

$$\sum M_x = I\frac{\ddot{y}_b - \ddot{y}_t}{l_b + l_t} + I_z\omega\frac{\dot{x}_t - \dot{x}_b}{l_b + l_t} + I_z\dot{\omega}\frac{x_t - x_b}{l_b + l_t} \quad (6)$$

$$\sum M_y = I\frac{\ddot{x}_t - \ddot{x}_b}{l_b + l_t} - I_z\omega\frac{\dot{y}_b - \dot{y}_t}{l_b + l_t} \quad (7)$$

where

$$\sum F_x = k_1 i_{tx} + k_3 i_{bx} + k_{13} x_t + k_{14} x_b \quad (8)$$

$$\sum F_y = k_2 i_{ty} + k_4 i_{by} + k_{15} y_t + k_{16} y_b \quad (9)$$

$$\sum M_x = k_4 i_{by} l_b - k_2 i_{ty} l_t + k_{17} y_t + k_{18} y_b \quad (10)$$

$$\sum M_y = k_1 i_{tx} l_t - k_3 i_{bx} l_b + k_{19} x_t + k_{20} x_b \quad (11)$$

$$k_{13} = k_5 + k_9 \text{ , } k_{14} = k_6 + k_{10} \quad (12)$$

$$k_{15} = k_7 + k_{11} \text{ , } k_{16} = k_8 + k_{12} \quad (13)$$

$$k_{17} = k_{11} l_{bp} - k_7 l_{tp} \text{ , } k_{18} = k_{12} l_{bp} - k_8 l_{tp} \quad (14)$$

$$k_{19} = k_5 l_{tp} - k_9 l_{bp} \text{ , } k_{20} = k_6 l_{tp} - k_{10} l_{bp} \quad (15)$$

The superscript " $\cdot$ " denotes differentiation with respect to time. Note that $l_b$ , $l_t$ is distance between center of gravity and active magnetic unit, $l_{bp}, l_{tp}$ is distance between center of gravity and passive magnetic unit and $m$ is mass of rotor. Also, cross-section radial and polar mass moment of inertia are indicated as $I$ and $I_z$ , and $\omega$ is rotating speed.

With the mathematical model obtained as above, one can then design a stabilizing levitation controller for the system. Here, the integral sliding mode control (ISMC) is adopted. The detail of the controller design is omitted here for brevity. In this study, all simulations are done by MATLAB/Simulink. The system parameters and geometric sizes are given in TABLE I, and the detailed information of magnetic bearings is listed in TABLE II. Moreover, it is assumed that the rotor begins to rotate at t=0.2s with the torque of 1Nm, and the damping coefficient will be neglected, so there are levitation phase and rotation phase. If the maximum of rotating speed is set to 10000rpm, implying that the battery is full, it requires 183.84 seconds and the total stored energy is $9.626\times10^4\,\mathrm{J}$ .

The initial states of simulation case are x(0)=[-3.53x10-4m 0 3.53x10-4m 0 3.53x10-4m 0 -3.53x10-4m]T. Note that two additional states are needed for ISMC, which are taken to be xm(0)=[0,0]T. The initial states for ISMC are thus [xm(0), x(0)]T. Moreover, the parameters of ISMC controller are listed on TABLE III, mainly provided by trial and error. The results of numerical simulation in duration of $t = 0 \sim 1\mathrm{sec}$ are shown in Fig. 10~13, including variation of rotating speed, trajectory and displacements of rotor at AMBs, and the control current $i_{bx}$, $i_{by}$, $i_{tx}$, $i_{ty}$ .

## V. CONCLUSIONS

In this paper, a novel type of active magnetic unit is proposed and applied to a ring-type flywheel battery system. The active magnetic unit consists of a conventional Halbach array with additional coil to actively adjust the magnetic force. The measurements of active and passive magnetic units with segmented Halbach array are analyzed. The flywheel energy storage system has been stabilized with ISMC controller. The illustrative example reveals that controller parameters are adequately adjusted to stabilize the unstable rotor. The robustness issue of suppressing the external disturbances and model uncertainties, such as assembly errors, manufacturing errors, mass unbalance and sensor noise, are further work scope. The fabrication and manufacturing of proposed flywheel battery prototype will be done in near future, and the experiment and development of driver of motor/generator are main work scope in next stage.

## ACKNOWLEDGMENT

This work is supported in part by the Ministry of Science and Technology of Taiwan, ROC, under the Grant NSC 102-2221-E-194 -026.

## REFERENCES

[1] Schweitzer, G. and Eric H. Maslen (Ed.), *Magnetic Bearing*, Springer-Verlag, Berlin Heidelberg, 2009.

[2] Schweitzer, G. Bleuler, H., and Traxler, A., *Active Magnetic Bearings*, Hochschleverlag AG an der ETH Zurich, 1994.

[3] Chow-Shing Toh and Shyh-Leh Chen, "Development of a Ring-type Flywheel Battery System for Storage of Renewable Energy," *The 13th International Symposium on Magnetic Bearing*, 2012, Arlington, Virginia, USA.

[4] S. Jinji, R. Yuan and F. Jiancheng, Passive axial magnetic bearing with Halbach magnetized array in

magnetically suspended control moment gyro application, *Journal of Magnetism and Magnetic Materials 323*, 2011, pp. 2103-2107
[5] Y.M. Choi, M.G. Lee, D.G. Gweon, and J. Jeong, A new magnetic bearing using Halbach magnet arrays for a magnetic levitation stage, *Review of scientific instruments 80*, 045106, 2009

TABLE I. PARAMETERS OF PROPOSED FLYWHEEL BATTERY PROTOTYPE

| $m$ (kg) | $I$ (kgm$^2$) | $I_z$ (kgm$^2$) |
|---|---|---|
| 19.62 | 0.1623 | 0.1756 |

| $l_b$ (m) | $l_t$ (m) | $l_{bp}$ (m) | $l_{tp}$ (m) |
|---|---|---|---|
| $9.794\times10^{-2}$ | $9.805\times10^{-2}$ | $4.112\times10^{-2}$ | $4.523\times10^{-2}$ |

TABLE II. PARAMETERS OF ACTIVE AND PASSIVE MAGNETIC BEARING

| | |
|---|---|
| Nominal air gap of AMB | $2\times10^{-4}$m |
| Nominal air gap of PMB | $2.5\times10^{-4}$m |
| Cross section of magnetic pole | $1.24\times10^{-3}$ m$^2$ |
| Number of coil turns | 270 |
| Width of permanent magnet, a | $5\times10^{-3}$m |
| Height of permanent magnet, b | $5\times10^{-3}$m |

TABLE III. PARAMETERS OF INTEGRAL SLIDING MODE CONTROLLER

| $b_1$ | $b_2$ | $\rho$ | $\alpha$ | $k_c$ | $\varepsilon$ |
|---|---|---|---|---|---|
| 50 | 150 | 5 | 2 | 0.7 | 0.5 |

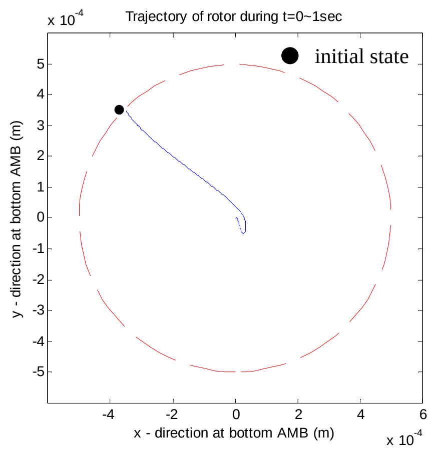


Fig. 10 Trajectory of rotor at bottom active magnetic bearing

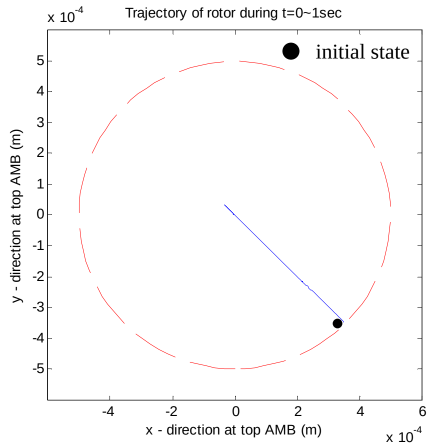


Fig. 11 Trajectory of rotor at top active magnetic bearing

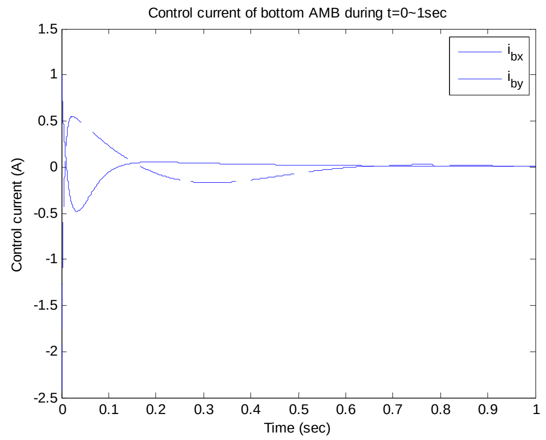


Fig. 12 Control current for $i_{bx}$ and $i_{by}$

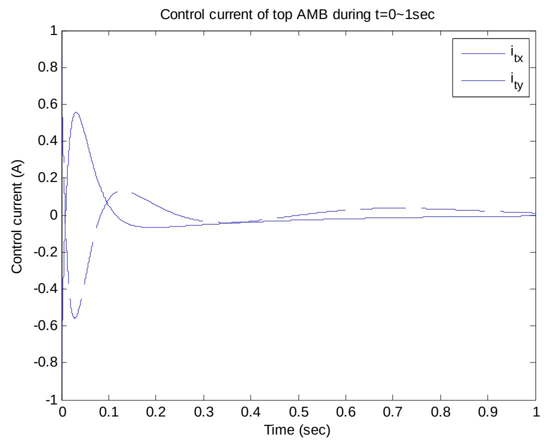


Fig. 13 Control current for $i_{tx}$ and $i_{ty}$